Undulations from amplified low frequency surface waves

Antonin Coutant*

Max Planck Institute for Gravitational Physics,

Albert Einstein Institute, Am Muhlenberg 1, 14476 Golm, Germany, EU

Renaud Parentani†

Laboratoire de Physique Théorique, CNRS UMR 8627,

Bâtiment 210, Université Paris-Sud 11, 91405 Orsay Cedex, France

(Dated: November 12, 2012)

We study the scattering of gravity waves in longitudinal stationary flows. When the flow velocity becomes supercritical, counterflow propagating waves are amplified in such a way that, in the zero-frequency limit, the free surface develops an undulation, i.e., a zero-frequency wave of large amplitude with nodes located at specific places. From this, we show that the unperturbed flat surface is unstable against perturbations of arbitrary small amplitude. We then show that this instability also appears when treating low frequency waves by a stochastic ensemble. The relation between the generation of undulations and black hole radiation (the Hawking effect) is discussed.

PACS numbers: 47.35.Bb, 04.70.Dy,

Keywords: Gravity Waves, Undulation, Analog Gravity, Hawking Radiation

*Electronic address: antonin.coutant@aei.mpg.de

†Electronic address: renaud.parentani@th.u-psud.fr

I. INTRODUCTION

It has long been observed that stationary flows over an obstacle which cross the speed of surface waves (Froude number $F_n = 1$) are often associated with an undulation, i.e. a zero-frequency wave with a macroscopic amplitude [1, 2]. In this paper we study a time dependent phenomenon which can be considered, in an appropriate zero-frequency limit, as a precursor of this phenomenon. We study the linear scattering of low frequency waves which propagate against a non turbulent and irrotational flow when the free surface does not already contain an undulation. When approaching the locus where $F_n = 1$ is crossed, these waves are blocked while their wave vector increases. Using the analogy with gravity [3–7], these flows correspond to white hole geometries, and the horizon is located where $F_n = 1$. To understand the scattering of waves on such flows one must take into account the dispersion relation of gravity waves. The relation between their frequency Ω (measured in the fluid frame) and their wave vector k is

$$\Omega^2 = c_{\rm gw}^2 F_{\rm gw}^2(k) = gk \tanh(h_B k), \tag{1}$$

where h_B the height of the background flow, and g the gravitational acceleration. In the usual case, when the conserved frequency ω (measured in the lab frame) is high enough, an incoming wave packet engenders two reflected waves which follow different trajectories, and which possesses different relative amplitudes. In the limit $\omega \to 0$, two unusual properties combine and produce a long lasting undulation with a large amplitude. One first finds that the two scattered waves merge and form a standing wave with nodes at definite places. Second, one finds that the amplification of this wave grows as $1/\omega$. This second aspect is directly related to the famous prediction of Hawking [8] according to which an incipient black hole should emit a steady thermal spectrum of photons, see [9, 10] for a pedagogical introduction and a review. In this sense black hole emission and the generation of undulations are based on a common amplification mechanism.

To demonstrate that free surfaces (which contain no undulation) are unstable with respect to initial conditions, we consider a series of wave packets with decreasing value of ω which all produce the same undulation. We show that the amplitude of the incoming wave linearly decreases in ω. Hence there is an instability at very low frequency. So far this concerns the scattering of initial wave packets. However, given that in realistic conditions low frequency waves are inevitably excited in an uncontrollable manner, a statistical treatment of incoming wave amplitudes is required. When using a thermal ensemble to characterize their statistical properties, the above amplification is further enhanced since the noise in a thermal bath grows as

$1/\omega$. This extra power of $1/\omega$ leads to a time dependent growth of the undulation amplitude [11–13]. The growth will continue until some mechanism, which could be due to nonlinearties or dissipation, will saturate it. These late time processes are not discussed in the present work.

It should be emphasized that similar phenomena occur in all dispersive media. In fact they are closely related to the appearance of the "layered structures" found in ^{4}He [14], and in Bose gases [15], when the flow exceeds the Landau critical velocity[1]. They also occur in atomic Bose Einstein condensates where the dispersion relation is $F^2_{\rm BEC} = k^2 + \xi^2 k^4/4$ instead of Eq. (1). In this paper, even though we have in mind gravity waves, we formulate the problem in terms which apply to the general case. Namely, our treatment depends on the dispersion relation F^2 which characterizes the medium, and quantities which characterize the background flow: the velocity of the flow, the speed of low wavenumber waves, and the fluid density.

II. ACTION FORMALISM AND WAVE EQUATION

We consider surface waves which propagate in a water tank of constant transverse dimension $L_\perp$. We assume that the flow is incompressible, non turbulent, and irrotational. We also assume that both the bottom of the tank and the background free surface do not depend on the transverse coordinate, and become asymptotically flat in the upstream region. We call $h_{\rm as}$ and $v_{\rm as}$ the asymptotic values of the water depth and the background flow velocity in this region. For simplicity, we only study waves with no dependence in the transverse coordinate[2], and we neglect the effects of capillarity. To incorporate them, one should consider the dispersion relation which generalizes Eq. (1) by including the capillary length [4].

When the background flow is stationary and non-uniform, the linear equation which governs the propagation of these waves is rather complicated [4, 7]. Yet, this equation can be derived from an action for the perturbations ϕ of the velocity potential. Moreover this action possesses a rather simple structure which is very similar to that of sound waves in an irrotational fluid [16]. As we shall see, the properties of the scattering of waves are efficiently described using the action formalism. The action has the following structure

$$S = \frac{1}{2}\int \rho(x)\left\{\frac{1}{c^2(x)}[(\partial_t + v_x(x)\,\partial_x)\phi]^2 + \phi\,\hat{F}^2(d_\Lambda(x))\,\phi\right\} dxdt. \qquad (2)$$

The function $\rho(x)$ is an effective 1-dimensional fluid density, $v_x(x)$ is the background flow velocity, $c(x)$ fixes the low frequency group velocity, and $\hat{F}^2$ is a differential operator which

[1] We are grateful to T. Jacobson to have drawn our attention to these works.
[2] Modes with a non zero transverse momentum $p_\perp$ are studied in [13].

governs the dispersion relation. The combination $\rho\hat{F}^2$ forms a self-adjoint operator, and $d_\Lambda(x)$ is the local dispersive wavelength. (In an atomic Bose condensate, the latter is known as the healing length [17, 18].) For each fluid, these functions are related in a specific manner to the properties of the background flow.

For gravity waves, assuming an incompressible fluid, i.e., a constant 3-dimensional density ρ_0^{3D}, there are several (physically equivalent) ways to identify these functions. Using [7][3] a convenient choice is

$$\hat{F}^2(d_\Lambda(x)) \;=\; \frac{1}{d_\Lambda(x)} i\partial_x \tanh(d_\Lambda(x) i\partial_x), \tag{3a}$$

$$d_\Lambda(x) \;=\; h_{\rm as}\frac{v_{\rm as}v_x(x)}{v^2(x)}, \tag{3b}$$

$$\rho(x) \;=\; \rho_0^{3D} L_\perp d_\Lambda(x), \tag{3c}$$

$$c^2(x) \;=\; d_\Lambda(x)\left[g + \partial_y(v^2/2)_{y=h_B(x)}\right] \doteq d_\Lambda(x)\, g_{\rm eff}(x). \tag{3d}$$

In the above, $v^2 = v_x^2 + v_y^2$, where v_x and v_y are the horizontal and vertical components of the background velocity, evaluated along the free surface $y = h_B(x)$. The quantity $g_{\rm eff}$ is the effective gravitational acceleration which takes into account the centrifugal acceleration. Asymptotically, all x dependence are negligible, and Eq. (3d) delivers the standard expression $c_{\rm as}^2 = h_{\rm as}g$. For long wavelengths, i.e. low gradients $kd_\Lambda \ll 1$, the dispersive length d_Λ drops out from Eq. (3a) and one gets the dispersionless expression $F^2 \to k^2$, since $k = -i\partial_x$. For smaller wavelengths, combining F^2 and c^2, one finds a generalized version of Eq. (1) where d_Λ acts as a dressed value of $h_{\rm as}$. In fact, to lowest order in $\partial_y v_x$, $d_\Lambda(x)$ reduces to the water depth at x.

As far as the scattering of waves is concerned, all is needed is the knowledge of the differential operator $\hat{F}^2$ and the functions ρ, v, c, d_Λ entering in Eq. (2). In other words, the intricate aspects of the above equations will play no role in the sequel. Yet, to make relevant physical predictions, one extra information is needed, namely, the relation between the velocity potential ϕ and some observable quantity. For gravity waves, the relevant observable is the vertical fluctuation of the surface $\delta h(t,x) = h(t,x) - h_B(x)$ with respect to the background free surface $y = h_B(x)$. The link between ϕ and δh is

$$\delta h(t,x) = -\frac{1}{g_{\rm eff}(x)}(\partial_t + v_x(x)\partial_x)\phi(t,x). \tag{4}$$

[3] In this work, Unruh derives the wave equation on stationary background flows using curvilinear coordinates. Here we re-express his results using horizontal and vertical cartesian coordinates x, y. The simplest way to obtain Eqs. (3), is to start from the wave equation in Eq. (113) and to use Eqs. (28),(29) to express ∂_ϕ in terms of ∂_x.

It is interesting to notice that δh is directly related to π, the momentum conjugated to ϕ, given the action of Eq. (2). Indeed one has

$$\pi(t,x) \doteq \frac{\rho(x)}{c^2(x)}(\partial_t + v_x(x)\partial_x)\phi(t,x), \tag{5a}$$

$$= -(\rho_0^{3D} L_\perp)\,\delta h(t,x). \tag{5b}$$

It is also interesting to notice also that for sound waves, e.g. in an atomic Bose condensate, the density fluctuation $\delta\rho$ is related to the momentum π, and the potential ϕ, by very similar equations, see Eq. B.11 in [18]. Therefore the forthcoming analysis also applies to these waves, when using the appropriate $\hat{F}^2$ operator governing dispersion.

The conserved Hamiltonian associated with Eq. (2) will play an important role in the sequel. It is given by

$$H = \frac{1}{2}\int \frac{\rho}{c^2}\left\{\left[\frac{c^2\pi}{\rho} - v_x\,\partial_x\phi\right]^2 + v_x^2(\partial_x\phi)^2 - c^2\,\phi\hat{F}^2(d_\Lambda)\phi\right\}dx. \tag{6}$$

The wave equation can then be obtained from Hamilton equations. The first equation $\partial_t\phi = \{\phi, H\}$, where $\{\,,\}$ is the Poisson bracket, gives Eq. (5a). The second equation, $\partial_t\pi = \{\pi, H\}$, gives

$$(\partial_t + \partial_x v_x(x))\pi(t,x) = \rho(x)\hat{F}^2(d_\Lambda(x))\,\phi(t,x), \tag{7}$$

which corresponds to Eq. (86) in [7]. Taken together, these equations give

$$\left[(\partial_t + \partial_x v_x(x))\frac{\rho(x)}{c^2(x)}(\partial_t + v_x(x)\partial_x) - \rho(x)\hat{F}^2(d_\Lambda(x))\right]\phi(t,x) = 0. \tag{8}$$

Using the fact that the co-moving frequency Ω is given by $\Omega = \omega - vk$, one verifies that the Hamilton-Jacobi equation associated with Eq. (8) (obtained by writing $\phi = e^{-i\omega t + i\int^x k_\omega dx'}$ and by working to lowest order in the spatial gradients) gives

$$\Omega^2 = (\omega - v_x(x)\,k_\omega(x))^2 = c^2(x)F^2(d_\Lambda(x)). \tag{9}$$

which generalizes Eq. (1) to non-uniform stationary flows.

A. Complete orthonormal mode basis

When considering stationary background flows, as in the present case, it is extremely useful to decompose the surface waves in terms stationary *complex* modes of the form $e^{-i\omega t}\phi_\omega(x)$. The spatial part $\phi_\omega(x)$ then obeys

$$\left[(\omega + i\partial_x v_x(x))\frac{\rho(x)}{c^2(x)}(\omega + iv_x(x)\partial_x) + \rho(x)F(d_\Lambda(x))\right]\phi_\omega(x) = 0. \tag{10}$$

These modes are useful because they form a complete basis for the real solutions of Eq. (8), and because they efficiently describe their scattering. For more explanations, we refer to [18, 19]. The notions of completeness and orthogonality are based on the conserved product associated with Eq. (2). For any pair ϕ_1, ϕ_2 of complex solutions of Eq. (8), the integral

$$(\phi_1|\phi_2) = i \int (\phi_1^* \pi_2 - \pi_1^* \phi_2) dx, \tag{11}$$

is constant, in virtue of Hamilton's equations. (This is true even when ρ, v, and c depend on time. When they are independent of time, the hamiltonian of Eq. (6) is another conserved quantity.) Several important properties concerning Eq. (11) should be mentioned.

First, when considering two stationary modes, their overlap vanishes when $\omega_1 \neq \omega_2$. This guarantees that the orthogonal ω-sectors do not mix with each other, and can thus be studied separately.

Second, the sign of the above product is *not* definite. In fact the norm of the complex conjugated $(e^{-i\omega t}\phi_\omega)^*$ is the opposite of that of $e^{-i\omega t}\phi_\omega$. To form a complete basis it is therefore sufficient to consider the set of positive norm modes together with their complex conjugated. Positive norm modes will be noted ϕ^a_ω, and negative norm ones $(\phi^a_\omega)^*$, where a is a discrete index which accounts for the dimensionality (discussed below) of the set of modes at fixed ω. As usual, it is appropriate to work with an orthonormal mode basis where all positive norm elements obey

$$(\phi^a_\omega|\phi^b_{\omega'}) = N\, \delta^{ab}\, \delta(\omega - \omega'), \tag{12}$$

where δ^{ab} is the Kronecker symbol, where $\delta(\omega - \omega')$ is the Dirac distribution (because the domain of x is the entire real axis), and where N is an arbitrary (real and positive) constant which has the dimension of an action. A possible choice for gravity waves which depends on the flow properties is

$$N_{\rm gw} = \rho_0^{3D} L_\perp \times h_{\rm as}^3 c_{\rm as} = \frac{\rho_0^{3D} L_\perp}{g \bar{N}^2}. \tag{13}$$

When using the scalar product (11) and the relation (5a), one verifies that $\bar{N} = h_{\rm as} c_{\rm as}^{3/2}$ is the 'net' amplitude of the modes (see Eq. (17) below), which guarantees that they are normalized as in (12).

Third, the set of modes at fixed $|\omega|$, i.e. the set $\{\phi^a_\omega, \phi^b_{-\omega}\}$ and their complex conjugated, can be alternatively organized according to the sign of the frequency $i\partial_t$. This re-arrangement is justified because modes with opposite values of $i\partial_t$ do not mix when propagating in a stationary flow. This means that $e^{-i\omega t}\phi^a_\omega$ will mix with $e^{-i\omega t}(\phi^b_{-\omega})^*$ but not with $e^{i\omega t}\phi^b_{-\omega}$. Therefore, in the

sequel, we shall work with the set $\{\phi^a_\omega, (\phi^b_{-\omega})^*\}$ which contains modes with norm of both signs. In the presence of dispersion, and/or in inhomogeneous flows, there is no relation between the sign of ω and that of the norm. Hence a case by case analysis is required to identify the various modes and their norm.

Fourth, when considering the real solutions of Eq. (8) which vanish asymptotically (for $x \to \pm\infty$), a complete basis is provided by the stationary modes ϕ_ω which are asymptotically bounded, i.e. stay finite as $x \to \pm\infty$. Hereafter we call them ABM, for asymptotically bounded mode. Importantly, the dimensionality of this set depends on the value of ω, and the properties of the flow. In what follows we consider flows which cross the speed of low frequency waves once, at a position conventionally put at $x = 0$, as described in Fig. 1. In this case, there are three ABM for $\omega < \omega_{\rm max}$, and only two for $\omega > \omega_{\rm max}$[4] The value of $\omega_{\rm max}$ is fixed by the condition that the line $\omega - v_{\rm as}k$ be tangent to the dispersion relation evaluated on the asymptotic right side, see Fig. 2. Above $\omega_{\rm max}$, we call the two orthogonal ABM by ϕ^V_ω and $(\phi^U_{-\omega})^*$, where the superscript U (V) indicates the sign of the group velocity *with respect to the fluid*: U (V) modes propagate against (with) the flow. Below $\omega_{\rm max}$, the three ABM are denoted ϕ^V_ω, $(\phi^U_{-\omega})^*$, and ϕ^U_ω, where the third one has a positive norm. Because we are interested in the low frequency limit, only the second set is relevant.

To simplify the presentation, in the sequel, we shall neglect the V-mode, and only consider the U-modes ϕ^U_ω, $(\phi^U_{-\omega})^*$ which are responsible for the undulation, and for the Hawking effect. However, as shown in [18, 20], the coupling between ϕ^V_ω and the U-modes is non negligible. Yet, it does not affect the low frequency behavior of the mode mixing between ϕ^U_ω and $(\phi^U_{-\omega})^*$: only some overall constants are affected. Since our purpose it to study the behavior of low frequency waves, we can, and shall, ignore the V-modes. Under this approximation, dropping the superfluous index U, any low frequency upstream moving wave can be decomposed as

$$\bar\phi(t,x) = 2{\rm Re}\left\{\int_0^{\omega_{\rm max}} e^{-i\omega t}\left[a_\omega\,\phi_\omega(x) + b_\omega\,(\phi_{-\omega}(x))^*\right]d\omega\right\}, \tag{14}$$

where $a_\omega = (e^{-i\omega t}\phi_\omega|\,\bar\phi)/N$ and $b_\omega = -(e^{-i\omega t}(\phi_{-\omega})^*|\,\bar\phi)/N$ are the constant components of $\bar\phi$ in the mode basis one has adopted, and where the minus sign in the last equation arises from the fact that $(\phi_{-\omega})^*$ is a negative norm mode.

Since the norm of Eq. (11) is identically zero for all real waves, it seems to be of small

[4] When the flow is everywhere subcritical $F_n < 1$, for the dispersion relation of Eq. (1), at fixed ω, there exist four ABM, two with positive norm, and two with a negative one, as can be seen from Fig. 2. When the flow everywhere supercritical, $F_n > 1$, there are two ABM with opposite norm.

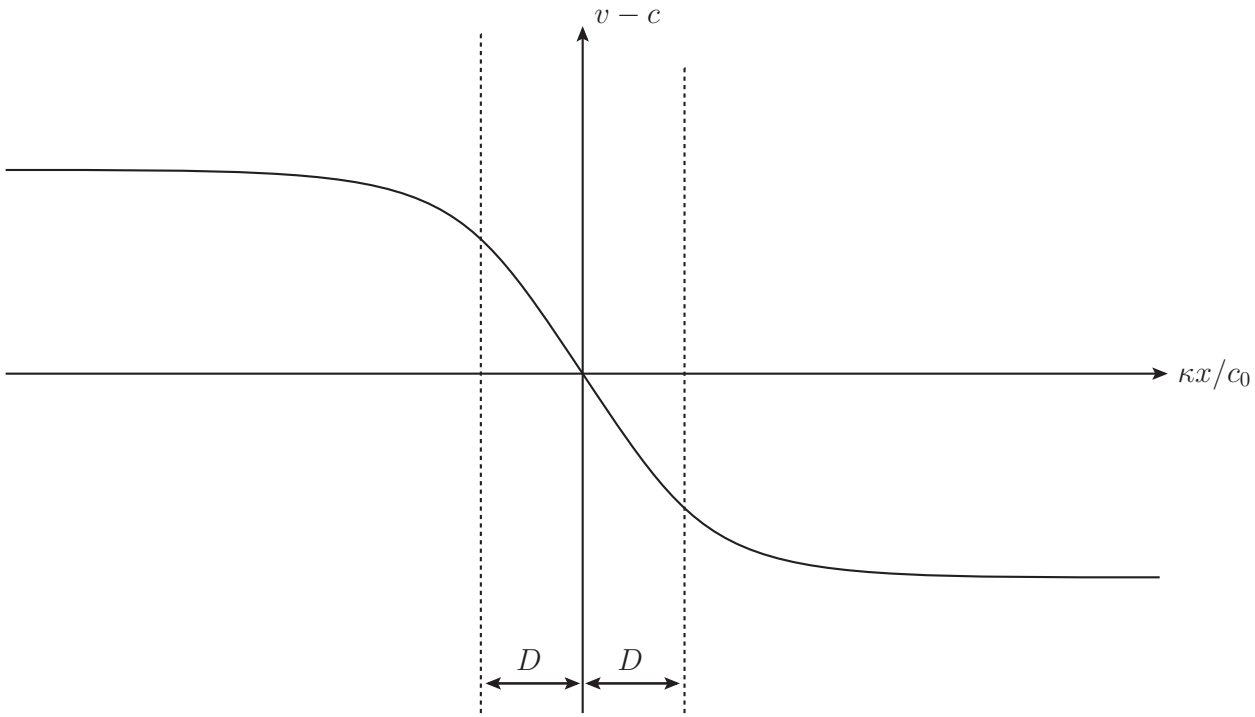

Figure 1: Background profile $v_x - c$ as a function of x with $v > 0$. The chosen profile is $v_x - c = -c_0 D \tanh(\kappa x/c_0 D)$, where c_0 is the speed at $x = 0$. The frequency κ is defined by $\partial_x (v_x - c)_{|x=0} = -\kappa$. In a gravitational context, this quantity corresponds to the surface gravity of the horizon [3]. The parameter D governs the extension of the near wave blocking region where $c - v_x \sim \kappa x$. On the asymptotic subcritical right side, $v_x(x)$ and $c(x)$ reach the constant values $v_{\rm as}$ and $c_{\rm as}$.

relevance for surface waves[5]. Similarly the sign of the frequency seems not well defined since both signs of $i\partial_t$ appear in real waves, both for the waves made with $a_\omega \phi_\omega$ or $b_\omega (\phi_{-\omega})^*$. To understand that there is a physically relevant, and important, information, let us consider the energy function. Using the mode normalization of Eq. (12), the energy transported by Eq. (14) is given by the value of Eq. (6) evaluated with $\phi = \bar{\phi}$:

$$\bar{E} = H\left[\bar{\phi}\right] = \frac{1}{2}(\bar{\phi}|i\partial_t\bar{\phi}) = N\int_0^{\omega_{\rm max}} \omega\left[|a_\omega|^2 - |b_\omega|^2\right] d\omega. \tag{15}$$

We first verify that the choice of N used in Eq. (12) drops out from the products $N|a_\omega|^2\omega d\omega$ and $-N|b_\omega|^2\omega d\omega$, which have the dimension of an energy. We also see that these products give the energy contribution of real waves described by ϕ_ω, and that of those described by

[5] The norm of Eq. (11) (with $N = \hbar$) is used in quantum field theory to decompose the field operator into creation and destruction operators which provide a particle interpretation to the field excitations [21, 22]. In the case of phonons in a Bose condensate, this is well defined and also physically relevant [17].

$\phi_{-\omega}$, respectively. (Hence working with the *positive norm* complex modes $\{\phi_\omega, \phi_{-\omega}\}$ to describe the real waves, the sign of the frequency of the complex modes fixes the sign of the energy of the corresponding waves. Equivalently, when working with the positive frequency mode set $\{\phi_\omega, (\phi_{-\omega})^*\}$, the sign of the mode norm fixes that of the wave energy.)

B. *S*-matrix description of waves scattering

The most efficient way to describe the scattering of low frequency waves in a stationary flow is to work at fixed ω, and to study how the two complex modes ϕ_ω and $(\phi_{-\omega})^*$ mix. As in any scattering, it is useful to introduce the two incoming modes $\phi^{\rm in}_\omega, (\phi^{\rm in}_{-\omega})^*$ which shall be scattered, and to relate them to the outgoing modes $\phi^{\rm out}_\omega, (\phi^{\rm out}_{-\omega})^*$ which have been scattered. Given that the flow is asymptotically uniform, the asymptotic properties of these four modes are easily found. Indeed, since the background functions v, c, ρ are all asymptotically constant, the solutions of Eq. (10) are superpositions of plane waves. Each plane wave is characterized by a constant wave number k_ω which is a real root of Eq. (9) evaluated asymptotically. The various roots are plotted on Fig.2. As explained earlier, we only consider those corresponding to waves

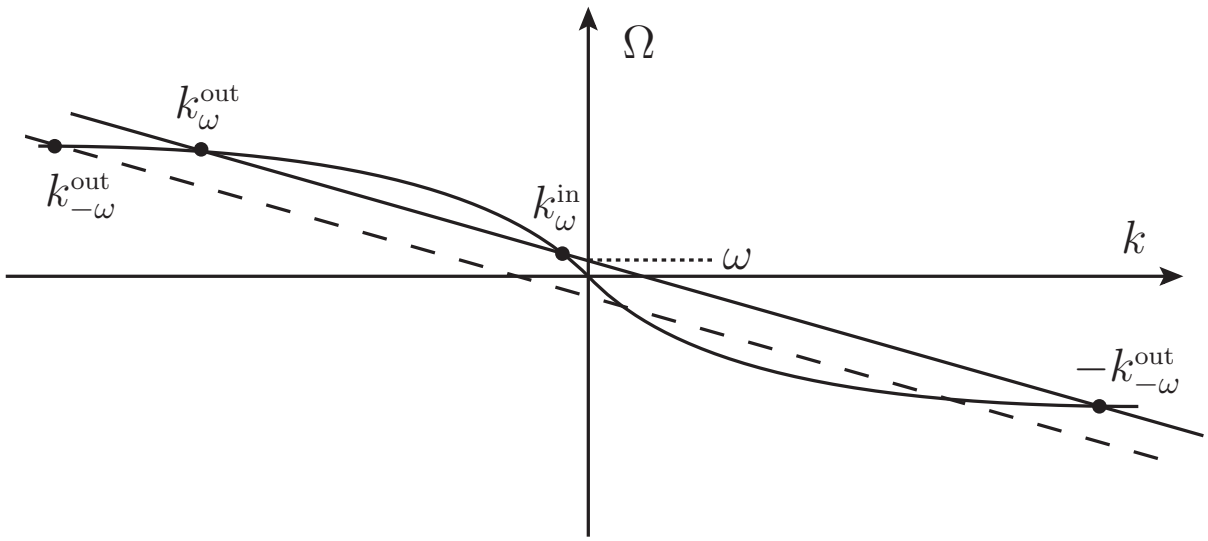

Figure 2: Dispersion relation, Ω versus k, on the asymptotic right side and for the counter-propagating waves with respect to the fluid. The continuous (dotted) straight line is $\omega - v_{\rm as}k$ of Eq. (9) evaluated asymptotically for $\omega > 0$ ($-\omega < 0$) while the curve is $c_{\rm as}F(k)$. Each intersection is thus a solution. The identification of three roots is described in the text. By comparing the straight and dotted lines, we see that $k^{\rm out}_{-\omega} > 0$ solves Eq. (9) for $-\omega < 0$, which means that $-k^{\rm out}_{-\omega}$ solves Eq. (9) for $\omega > 0$. When considering the limit $\omega \to 0$, $k^{\rm out}_\omega$ and $k^{\rm out}_{-\omega}$ merge and define k_Z of Eq. (16a).

moving upstream (with respect to the fluid, not the laboratory frame). On the asymptotic right side, where $0 < v_{\rm as} < c_{\rm as}$, they are three real roots. The low wave-vector one describes the incoming mode, whereas the two high wave-vector roots describe the outgoing modes. For $\omega \to 0$, these roots reach equal and opposite values $\pm k_Z$. Indeed to first order in ω one has

$$k_\omega^{\rm out} \sim k_Z + \omega/v_g^Z, \tag{16a}$$

$$k_\omega^{\rm in} \sim -\frac{\omega}{c_{\rm as} - v_{\rm as}} = \omega/v_g^{\rm in}, \tag{16b}$$

where $v_g^Z > 0$ is the group velocity $v_g = (\partial_\omega k)^{-1}$ evaluated asymptotically and for $\omega \to 0$. In the second line one verifies that the in mode is propagating to the left since $v_g^{\rm in} = -c_{\rm as} + v_{\rm as} < 0$. On the other side of the blocking region, for $x \to -\infty$ where $v > c$, there is only one real root, which corresponds to the negative root $-k_{-\omega}^{\rm in}$. To each root, there exists an asymptotic solution of the wave equation which can be normalized using Eq. (11). Of crucial importance, the norm sign of these modes is not the same. In fact, as we see from Eqs. (5a) and (11), this sign coincides with that of the co-moving frequency $\Omega = \omega - vk$. Hence, for $\omega > 0$, the two positive roots $k_\omega^{\rm in}$ and $k_\omega^{\rm out}$ describe the *in* and *out* positive norm modes, whereas $-k_{-\omega}^{\rm in}$ and $-k_{-\omega}^{\rm out}$ describe the *in* and *out* negative norm modes. Explicitly, using $\bar{N}$ of Eq. (13), the asymptotic positive and negative norm modes are

$$\varphi_\omega^a = \bar{N} \frac{e^{ik_\omega^a x}}{\sqrt{4\pi |\Omega(k_\omega^a) v_g^a|}}, \tag{17a}$$

$$(\varphi_{-\omega}^a)^* = \bar{N} \frac{e^{-ik_{-\omega}^a x}}{\sqrt{4\pi |\Omega(k_\omega^a) v_g^a|}}, \tag{17b}$$

where the exponent a stands for *in* and *out*. (For $(\varphi_{-\omega}^{\rm in})^*$, $h_{\rm as}$ and $c_{\rm as}$ should be evaluated on the left side when computing $k_{-\omega}^{\rm in}$ and $v_g^{\rm in}$, since this mode comes from that side.)

We now define the globally defined *in* and *out* modes using the standard procedure [10], e.g., the positive ingoing mode $\phi_\omega^{\rm in}$ is the solution of Eq. (10) which asymptotes in the past (in the sense of a broad wave packet) to $\varphi_\omega^{\rm in}$. We use the symbol φ to designate the asymptotic plane waves of Eq. (17), and ϕ the corresponding globally defined solutions. Since the two *in* modes, and the two *out* modes, form a basis of the ABM solutions of Eq. (10), they are related by a linear transformation which defines the S-matrix

$$\begin{pmatrix} \phi_\omega^{\rm in} \\ (\phi_{-\omega}^{\rm in})^* \end{pmatrix} = \begin{pmatrix} \alpha_\omega & \beta_\omega \\ \tilde{\beta}_\omega & \tilde{\alpha}_\omega \end{pmatrix} \cdot \begin{pmatrix} \phi_\omega^{\rm out} \\ (\phi_{-\omega}^{\rm out})^* \end{pmatrix}. \tag{18}$$

The fact that in each basis the two modes have opposite norm implies that the coefficients obey the anomalous scattering relation $|\alpha_\omega|^2 - |\beta_\omega|^2 = |\tilde{\alpha}_\omega|^2 - |\tilde{\beta}_\omega|^2 = 1$. Since $|\alpha_\omega| > 1$, the

scattering thus leads to an amplification of the waves [5, 6, 23, 24]. In addition, in the limit $\omega \to 0$, it can be shown that the amplification becomes very large, that is

$$|\alpha_\omega| \sim |\beta_\omega| \gg 1. \tag{19}$$

As we shall see, this is a crucial ingredient for the undulation. In [20] it was shown that, irrespectively of the smoothness of the profile near Froude number $F_n = 1$, the coefficients diverge as

$$|\alpha_\omega|^2 \sim |\beta_\omega|^2 \sim \frac{\bar{\kappa}}{2\pi\omega}. \tag{20}$$

When the profile is smooth, i.e. when $\kappa d_\Lambda/c_0 \ll 1$, one finds the Hawking result, i.e. $\bar{\kappa} = \kappa$ where κ is the surface gravity defined in the caption of Fig. 1. When the profile is so abrupt that the inequality is not satisfied, $\bar{\kappa}$ is smaller than κ and determined by the dispersive length d_Λ. To characterize the phase of the coefficients we write them as

$$\alpha_\omega \sim |\alpha_\omega| e^{i(\theta+\theta')} \qquad \text{and} \qquad \beta_\omega \sim |\alpha_\omega| e^{i(\theta'-\theta)}, \tag{21}$$

such that θ is half the phase of $\alpha_\omega \beta^*_\omega$, and θ' a common phase. As we shall see, θ participates to the determination of the location of the undulation nodes.

III. SCATTERING OF WAVE PACKETS

A. Incoming waves

We consider a series of incoming wave packets of positive energy, sent from the right side against the flow. Using the *in* modes basis $\phi^{\rm in}_\omega$, $(\phi^{\rm in}_{-\omega})^*$, this means that we set $b_\omega = 0$ in Eq. (14). To get explicit expressions, we work with

$$a_\omega = \frac{A}{n^{1/2}_{\bar{\omega}}} \exp\left(-\frac{(\omega-\bar{\omega})^2}{2\sigma_0^2\bar{\omega}^2}\right), \tag{22}$$

where A is a complex dimensionless amplitude $A = |A|e^{i\delta}$, and where the packets are normalized by

$$\int_0^{\omega_{\rm max}} |a_\omega|^2 d\omega = |A|^2. \tag{23}$$

We also assume that the waves are almost monochromatic. Irrespectively of the value of $\bar{\omega}$, this is realized if

$$\sigma_0 \ll 1. \tag{24}$$

In this regime, one finds $n_{\bar{\omega}} = \sigma_0 \bar{\omega} \pi^{1/2}$. The absence of any ω-dependent phase in Eq. (22) guarantees that the packets are all centered around $x = 0$ at $t = 0$.

We now analyze the early properties of this series of waves. Using the asymptotic behavior of $\phi_\omega^{\rm in}$ given in Eq. (17) we get

$$\bar{\phi}(x, t \to -\infty) = 2\mathrm{Re}\left\{ \bar{N} A \int_0^\infty e^{-\frac{(\omega-\bar{\omega})^2}{2\sigma_0^2\bar{\omega}^2}} \frac{e^{-i(\omega t - k_\omega^{\rm in} x)}}{\sqrt{4\pi\omega c_{\rm as}}} \frac{d\omega}{n_\sigma^{1/2}} \right\}. \tag{25}$$

In the broad wave regime of Eq. (24), we can accurately evaluate the integral with a saddle point approximation. Then, using Eq. (4) asymptotically, where $g_{\rm eff} = g$, the corresponding incoming height variation is

$$\delta\bar{h}^{\rm in}(x) \sim \delta\bar{h}_A^{\rm in} \times \sin\left(\bar{\omega} t - k_{\bar{\omega}}^{\rm in} x + \delta\right) e^{-\frac{\sigma_0^2\bar{\omega}^2}{2}(t - x/v_g^{\rm in})^2}, \tag{26}$$

where the amplitude is

$$\delta\bar{h}_A^{\rm in} = |A|\bar{N}\frac{\bar{\omega} h_{\rm as}}{c_{\rm as} - v_{\rm as}}\sqrt{\frac{2\sigma_0}{\pi^{1/2} c_{\rm as}^3}}. \tag{27}$$

As expected, the incoming wave (26) oscillates at a frequency $\bar{\omega}$, has a wavenumber $k_{\bar{\omega}}^{\rm in}$, and its envelope is propagating toward the wave blocking region at a speed $v_g^{\rm in} < 0$. We see that the argument of A, the phase δ, governs the precise initial positions of the nodes. We also see that at fixed A, its amplitude $\bar{\delta}h^{\rm in}$ decreases linearly for with $\bar{\omega}$. In this respect, it is also instructive to evaluate the conserved energy transported by the wave packet of Eq. (25). Using Eq. (15), one finds

$$\bar{E} = 2\bar{\omega} N |A|^2. \tag{28}$$

At fixed A, this energy is also arbitrary small in the limit $\bar{\omega} \to 0$.

B. Outgoing waves

At a time near $t = 0$, the waves of Eq. (25) reach the wave blocking region, around $x = 0$. There, they undergo a nontrivial scattering which is completely governed by Eq. (18). Because of this mode mixing, two outgoing wave packets are generated and propagate to the right. To analyze these two waves, it is convenient to introduce the complex wave $\bar{\phi}_{\mathbb{C}}$, defined by $\bar{\phi} = 2\mathrm{Re}(\bar{\phi}_{\mathbb{C}})$ in Eq. (14). At late time, using the *out* mode basis and Eq. (18), one finds

$$\bar{\phi}_{\mathbb{C}}(x, t \to +\infty) = \bar{\phi}_{\mathbb{C}}^{+}(t, x) + \bar{\phi}_{\mathbb{C}}^{-}(t, x). \tag{29}$$

where the two waves are

$$\bar{\phi}_{\mathbb{C}}^{+}(x, t \to +\infty) \;=\; \bar{N} A \int \alpha_\omega e^{-\frac{(\omega-\bar{\omega})^2}{2\sigma_0^2\bar{\omega}^2}} \frac{e^{-i(\omega t - k_\omega x)}}{\sqrt{4\pi|\Omega_{\rm out} v_g^{\rm out}|}} \frac{d\omega}{n_\sigma^{1/2}}, \tag{30a}$$

$$\bar{\phi}_{\mathbb{C}}^{-}(x, t \to +\infty) \;=\; \bar{N} A \int \beta_\omega e^{-\frac{(\omega-\bar{\omega})^2}{2\sigma_0^2\bar{\omega}^2}} \frac{e^{-i(\omega t + k_{-\omega} x)}}{\sqrt{4\pi|\Omega_{\rm out} v_g^{\rm out}|}} \frac{d\omega}{n_\sigma^{1/2}}. \tag{30b}$$

where $\Omega_{\rm out} = \Omega(k_\omega^{\rm out})$ is the co-moving frequency of the outgoing modes, and $v_g^{\rm out}$ their group velocity. Evaluated through a saddle point method, one obtains

$$\bar\phi^+_{\mathbb{C}}(x, t\to+\infty) \;\sim\; A_{\bar\omega}\,\alpha_{\bar\omega}\,\varphi^{\rm out}_{\bar\omega} e^{-i\bar\omega t}\, e^{-\frac{\sigma_0^2\bar\omega^2}{2}(t-x/v_g^{\rm out})^2}, \tag{31a}$$

$$\bar\phi^-_{\mathbb{C}}(x, t\to+\infty) \;\sim\; A_{\bar\omega}\,\beta_{\bar\omega}\,(\varphi^{\rm out}_{-\bar\omega})^* e^{-i\bar\omega t}\, e^{-\frac{\sigma_0^2\bar\omega^2}{2}(t-x/v_g^{\rm out})^2}, \tag{31b}$$

where their common amplitude factor $A_{\bar\omega}$ is given by

$$A_{\bar\omega} = A\sqrt{2\sigma_0\bar\omega\pi^{1/2}}. \tag{32}$$

We now have all the ingredients to consider the limit $\bar\omega \to 0$, keeping σ_0 constant. Using Eq. (21), the two outgoing waves merge to give a (real) zero-frequency wave of fixed profile, i.e.

$$\alpha_{\bar\omega}\,\varphi^{\rm out}_{\bar\omega} e^{-i\bar\omega t} + \beta_{\bar\omega}\,(\varphi^{\rm out}_{-\bar\omega})^* e^{-i\bar\omega t} \underset{\bar\omega\to 0}{\sim} 2|\alpha_{\bar\omega}| e^{i(\delta+\theta')}\Phi_U(x), \tag{33}$$

where

$$\Phi_U(x) \doteq \mathrm{Re}\left\{e^{i\theta}\phi_0^{\rm out}(x)\right\}, \tag{34}$$

gives the profile of the undulation. Since asymptotically $\phi_0^{\rm out}(x)$ is given by Eq. (17), we get

$$\Phi_U(x) = \bar N \frac{\cos\left(k_Z x+\theta\right)}{\sqrt{4\pi v_{\rm as} k_Z v_g^Z}}. \tag{35}$$

We see that this profile is independent of t, $\bar\omega$, and δ. Using Eq. (33), the outgoing real wave neatly factorizes and takes the simple form

$$\bar\phi(x, t\to+\infty) \sim 4\,|A_{\bar\omega}\alpha_{\bar\omega}|\cos(\delta+\theta')\times\Phi_U(x) e^{-\frac{\sigma_0^2\bar\omega^2}{2}(t-x/v_g^Z)^2}. \tag{36}$$

Since the slow varying envelope becomes a constant when $\bar\omega \to 0$, the outgoing signal becomes a standing wave with nodes at fixed locations. This is our first result.

To discuss the amplitude in physical terms, we compute the corresponding fluctuation of the free surface. Using Eq. (4), the undulation profile of δh_U associated with Eq. (35) is

$$\delta h_U(x) \doteq -\frac{v_{\rm as}}{g}\partial_x\Phi_U(x) \sim h_{\rm as}\bar N\sqrt{\frac{v_{\rm as}k_Z}{4\pi\bar N c_{\rm as}^4 v_g^Z}}\sin\left(k_Z x+\theta\right). \tag{37}$$

Similarly, the surface wave associated with the packet of Eq. (36) is

$$\delta\bar h^{\rm out}(x) \sim \delta\bar h^{\rm out}\sin\left(k_z x+\theta\right) e^{-\frac{\sigma_0^2\bar\omega^2}{2}(t-x/v_g^Z)^2}, \tag{38}$$

where the amplitude is

$$\delta\bar h^{\rm out} = h_{\rm as}\bar N\sqrt{\frac{4\Omega_{\rm out}}{\pi v_g^Z c_{\rm as}^4}}|A_{\bar\omega}\alpha_{\bar\omega}|\cos\left(\delta+\theta'\right). \tag{39}$$

To get rid of the dependence on the amplitude $|A|$ and the normalization $\bar{N}$, we compute the amplification factor. Using Eqs. (27) and (39), we find

$$\frac{\delta\bar{h}^{\rm out}}{\delta\bar{h}^{\rm in}} = \frac{(c_{\rm as}-v_{\rm as})}{\bar{\omega}}\sqrt{\frac{v_{\rm as}k_Z\bar{\kappa}}{2\pi c_{\rm as}v_g^Z}}\cos\left(\delta+\theta'\right). \tag{40}$$

Irrespectively of any choice, we see that the ratio diverges as $1/\bar{\omega}$ for $\bar{\omega}\to 0$. This is our second result. We also see that the amplitude of the undulation critically depends on the cosine in (40) whose value is fixed by δ. In practice, this phase is hard to control with precision. We learn here that the resulting amplitude is drastically affected by a small change of initial conditions. Hence, unless one knows the initial conditions with an arbitrary precision, one is *not* able to predict what will be the amplitude of the undulation. The unpredictable character of the undulation amplitude (in the linear regime) is our third result. This property becomes even clearer when the state of incoming waves is a statistical ensemble.

Before studying this, we make three extra comments which lead to specific predictions which could hopefully be tested in future experiments.

First, we emphasize that the linear treatment we used predicts that both signs of the amplitude are equally possible, since the sign is governed by the $\cos(\delta+\theta')$ of Eq. (40).

Second, to be more specific, we suppose that $v_{\rm as}\ll c_{\rm as}$. This means that we work with deep water waves. It simplifies the expressions and is relevant for many experiments. In this case, using Eq. (16a), we have

$$k_Z = \frac{c_{\rm as}^2}{h_{\rm as}v_{\rm as}^2} \qquad \text{and} \qquad v_g^Z = v_{\rm as}/2. \tag{41}$$

Hence the net amplification factor of Eq. (40) becomes

$$\frac{\delta\bar{h}_A^{\rm out}}{\delta\bar{h}_A^{\rm in}} = \frac{c_{\rm as}^2}{\bar{\omega}}\sqrt{\frac{\bar{\kappa}}{\pi h_{\rm as}v_{\rm as}}}\cos\left(\delta+\theta'\right). \tag{42}$$

We see that the amplification grows as $1/\sqrt{v_{\rm as}}$ for $v_{\rm as}\to 0$. This growth will be regulated by capillary effects.

Third, the phase θ which governs the location of the asymptotic nodes in Eq. (37) is complicated to compute because it accounts for the propagation from the blocking region to the asymptotic region. On the contrary, the undulation profile has a rather universal behavior near the blocking region, where $v_x - c \sim -\kappa x$, that is, for $|\kappa x| \ll D$ (see Fig 1). In addition we restrict our attention to the region where $k_\omega \lesssim 1/d_\Lambda$ (i.e., $|\kappa x| \lesssim 1$), meaning that one can approximate $F^2(k)$ in Eq. (9) by $k^2 - d_\Lambda^2 k^4/3$. In this region, using the results of [12] and Eq. (4), up to an overall constant factor, we get

$$\delta h_U(x) \propto {\rm Ai}\left(-x/d_{\rm broad}\right), \tag{43}$$

where Ai is the standard Airy function [25], and where the effective length is given by

$$d_{\rm broad} = \left(\frac{c_0 d_\Lambda^2(0)}{6\kappa} \right)^{1/3} . \tag{44}$$

This length depends both the on dispersive length $d_\Lambda(0) \sim h_B(0)$, the height of the flow near the blocking point, and the gradient $\kappa = \partial_x(v_x - c)$ evaluated at that place[6]. In agreement with the results of [12, 27, 28], this *broadening* length governs the behavior of the undulation near the blocking point. We also note that the velocity potential Φ_U of Eq. (34) is not described by an Airy function, but by its primitive integral. We finally note that these results also apply to undulations (of density fluctuation) found in Bose condensates where the dispersion is anomalous: $F^2_{\rm BEC} = k^2 + \xi^2 k^4/4$. In that case, $d_\Lambda(0)$ is related to the healing length ξ by $d_\Lambda(0) = \sqrt{3}\xi/2$, and the undulation lives where the flow is supercritical.

IV. STOCHASTIC ENSEMBLE

In realistic conditions, low frequency modes are excited in a non controllable manner. To describe in simple terms this randomness, we assume that the incoming waves are characterized by a thermal ensemble, i.e. with a noise growing like $1/\omega$ for $\omega \to 0$. To describe this distribution, one must use the field decomposition of Eq. (14) in terms of *in* modes where the coefficients a_ω and b_ω are random variables [29]. One sees again the usefulness of the mode basis. Such a Gaussian ensemble is defined by

$$\langle a_\omega \rangle = 0, \qquad \langle a^*_{\omega'} a_\omega \rangle = n^a_\omega \delta(\omega - \omega'), \tag{45a}$$

$$\langle b_\omega \rangle = 0, \qquad \langle b^*_{\omega'} b_\omega \rangle = n^b_\omega \delta(\omega - \omega'), \tag{45b}$$

where the two variables are independent, i.e. $\langle b^*_{\omega'} a_\omega \rangle = 0$. In a thermal state at temperature T, each monochromatic wave behaves as a (classical) harmonic oscillator in a thermal bath. However, since positive and negative energy modes respectively come from the right (R) and left (L) asymptotic regions, they will not share the same temperature. Moreover, their comoving frequency $\Omega = \omega - vk$ is Doppler shifted by the right or left asymptotic values of the flow velocity, see [18] for a discussion about thermal states in fluid flows. To take both effects

[6] The evaluation of $d_{\rm broad}$ is most easily done by considering the dispersion relation (9) with $F^2 \sim k^2 - d_\Lambda^2 k^4/3$ and $c - v_x \sim \kappa x$. One obtains $\kappa x \sim c_0 k^2 d_\Lambda^2/6$, then using $x = i\partial_k$, the mode in k-space is $\exp(i d^3_{\rm broad} k^3/3)$. Using a similar reasoning, one obtains the (ω-dependent) broadening length of [26] for deep water waves with non vanishing frequency ω.

into account, we parameterize the low frequency powers as

$$n^a_\omega = \frac{k_B T_R}{N\omega}, \tag{46a}$$

$$n^b_\omega = \frac{k_B T_L}{N\omega}. \tag{46b}$$

In this state, the average value of the surface perturbation vanishes, i.e.

$$\langle \delta h(t,x) \rangle = 0. \tag{47}$$

This is easily understandable using the wave packet analysis of the preceding section. Indeed, in a thermal state, initial phases (i.e. δ in Eq. (26) for the incoming waves) are random. Hence when averaging over δ in Eq. (38), the mean value vanishes. On the other hand, $\langle (\delta h(t,x))^2 \rangle$, the spread of δh is non trivial. To compute it, we use the mode decomposition (14) together with the distribution (45) for the coefficients a_ω, b_ω. By a calculation similar to that of Eq. (33), and using the profile δh_U of Eq. (37), one finds[7]

$$\langle (\delta h(t,x))^2 \rangle = 8 \int_0 (n^a_\omega + n^b_\omega) |\alpha_\omega|^2 d\omega \times \left(\delta h_U(x)\right)^2 . \tag{48}$$

This expression shows that the profile of the undulation is fixed and given in Eq. (37). In other words, the relative amplitude and the position of the nodes are not subjected to any randomness. On the other hand, its amplitude is a stochastic variable whose spread is fixed by the above expression. Therefore, the linearized treatment predicts that there is a high probability of observing a macroscopic undulation, with equal probability to find either sign. (Using Eq. (46), we verify that the choice of N in Eq. (13) enters in δh_U of Eq. (37) so that the spread of Eq. (48) is independent of N.)

In addition, when integrating over low frequencies, the integral which fixes the spread of the amplitude diverges since its integrand behaves as $1/\omega^2$. To regulate it, we consider a flow which has been formed for a finite amount of time t. Since it is impossible to distinguish frequencies below $\sim 1/t$, we introduce a low frequency cut-off on the integral in Eq. (48) and consider

$$\int_{1/t} (n^a_\omega + n^b_\omega) |\alpha_\omega|^2 d\omega \sim \frac{k_B (T_R + T_L)}{2\pi N} \bar{\kappa} t. \tag{49}$$

We see that the diverging character for low frequencies engenders a linear growth in time. (This result has been confirmed by numerical simulations in atomic Bose condensates [11].) We also see that the low frequency waves coming from the right and the left both contribute, with

[7] For more details, we refer to the Chapter 4 of [30], which presents results from [12, 13].

their respective powers given in Eq. (46). Of course, the amplitude of the undulation will grow linearly in time only as long as one can neglect nonlinearities, dissipation, or an infrared cut-off as in the case of transverse modes [13]. Ultimately, these will alter the picture and saturate the growth of the amplitude.

V. CONCLUSIONS

In this paper we studied the scattering of low frequency waves in supercritical flows when the stationary free surface is flat. In the zero-frequency limit, we showed that the outgoing reflected waves possess very specific properties. First, the two outgoing waves merge and form a single wave with a fixed spatial profile and nodes at specific places, see Eq. (33). Second, the amplification factor relating the amplitude of the incoming and outgoing waves diverges as the inverse of the conserved frequency, see Eq. (40). Third, this factor also depends on a combination of phases which renders the outcome effectively unpredictable, see the $\cos(\delta + \theta')$, where δ is given in Eq. (26) and θ' in Eq. (21). Fourth, we show that near the blocking point the profile of the undulation is given by an Airy function governed by a composite length scale formed with the dispersive length d_Λ and the gradient of the flow κ, see Eq. (44).

These properties tell us that free surfaces (which contain no undulation) are unstable when sending low frequency incoming waves, and that the large and unpredictable amplitude of the undulation is an expression of this instability. To account for this unpredictable character, in the last part of this article, we computed the averaged properties of undulations when the low frequency incoming waves are described by a statistical ensemble. In agreement with [11–13], we found in Eq. (48) that the undulation spatial profile is not subject to any randomness while its amplitude is a random quantity. In addition, the spread of this amplitude diverges for very low frequencies. This divergence is regulated when considering that the stationary flow only existed for a finite lapse of time. The linear treatment predicts a growth which is linear in this lapse. It would be interesting to experimentally test this prediction, as that concerning the profile of the undulation given in Eq. (43).

The low frequency divergence should also be regulated when including nonlinear effects. In this respect it would be particularly interesting to understand the transition from a growing undulation whose amplitude is a random variable to a saturated amplitude which is deterministically fixed by nonlinear equations. This question is relevant for both classical fluids and quantum ones, such as dilute atomic Bose gazes.

Acknowledgments

We are grateful to Germain Rousseaux for suggestions and interesting remarks.

---

[1] R. Johnson, *A modern introduction to the mathematical theory of water waves*, vol. 19. Cambridge University Press, 1997.

[2] G. Lawrence, "Steady flow over an obstacle," *J. Hydraul. Eng.* **113** no. 8, (1987) 981–991.

[3] W. Unruh, "Experimental black hole evaporation," *Phys. Rev. Lett.* **46** (1981) 1351–1353.

[4] R. Schutzhold and W. G. Unruh, "Gravity wave analogs of black holes," *Phys. Rev.* **D 66** (2002) 044019, arXiv:gr-qc/0205099 [gr-qc].

[5] G. Rousseaux, C. Mathis, P. Maissa, T. G. Philbin, and U. Leonhardt, "Observation of negative phase velocity waves in a water tank: A classical analogue to the Hawking effect?," *New J.Phys.* **10** (2008) 053015, arXiv:0711.4767 [gr-qc].

[6] S. Weinfurtner, E. W. Tedford, M. C. Penrice, W. G. Unruh, and G. A. Lawrence, "Measurement of stimulated Hawking emission in an analogue system," *Phys. Rev. Lett.* **106** (2011) 021302, arXiv:1008.1911 [gr-qc].

[7] W. Unruh, "Irrotational, two-dimensional Surface waves in fluids," arXiv:1205.6751 [gr-qc].

[8] S. Hawking, "Particle Creation by Black Holes," *Commun. Math. Phys.* **43** (1975) 199–220.

[9] R. Parentani and P. Spindel, "Hawking radiation," *Scholarpedia* **6** no. 12, (2011) 6958. http://www.scholarpedia.org/article/Hawking_radiation.

[10] R. Brout, S. Massar, R. Parentani, and P. Spindel, "A Primer for black hole quantum physics," *Phys. Rept.* **260** (1995) 329–454, arXiv:0710.4345 [gr-qc].

[11] C. Mayoral, A. Recati, A. Fabbri, R. Parentani, R. Balbinot, and I. Carusotto, "Acoustic white holes in flowing atomic Bose-Einstein condensates," *New J. Phys.* **13** (2011) 025007, arXiv:1009.6196 [cond-mat.quant-gas].

[12] A. Coutant, R. Parentani, and S. Finazzi, "Black hole radiation with short distance dispersion, an analytical S-matrix approach," *Phys. Rev.* **D 85** (2012) 024021, arXiv:1108.1821 [hep-th].

[13] A. Coutant, A. Fabbri, R. Parentani, R. Balbinot, and P. Anderson, "Hawking radiation of massive modes and undulations," *Phys. Rev.* **D 86** (2012) 064022, arXiv:1206.2658 [gr-qc].

[14] L. P. Pitaevskii, "Layered structure of superfluid 4 he with supercritical motion," *JETP Lett* **39** no. 9, (1984) 423–425.

[15] G. Baym and C. J. Pethick, "Landau critical velocity in weakly interacting bose gases," 1206.7066. http://arxiv.org/abs/1206.7066.

[16] R. Balbinot, A. Fabbri, S. Fagnocchi, and R. Parentani, "Hawking radiation from acoustic black holes, short distance and back-reaction effects," *Riv. Nuovo Cim.* **28** (2005) 1–55, arXiv:gr-qc/0601079 [gr-qc].

[17] F. Dalfovo, S. Giorgini, L. P. Pitaevskii, and S. Stringari, "Theory of Bose-Einstein condensation in trapped gases," *Rev. Mod. Phys.* **71** (1999) 463–512.

[18] J. Macher and R. Parentani, "Black hole radiation in Bose-Einstein condensates," *Phys. Rev.* **A 80** (2009) 043601, arXiv:0905.3634 [cond-mat.quant-gas].

[19] A. Coutant and R. Parentani, "Black hole lasers, a mode analysis," *Phys. Rev.* **D 81** (2010) 084042, arXiv:0912.2755 [hep-th].

[20] S. Finazzi and R. Parentani, "Hawking radiation in dispersive theories, the two regimes," *Phys.Rev.* **D85** (2012) 124027, arXiv:1202.6015 [gr-qc].

[21] S. Weinberg, *The Quantum Theory of Fields, Vol. 1: Foundations*, vol. 1. Cambridge University Press, 1995.

[22] R. Wald, *General relativity*. University of Chicago press, 1984.

[23] U. Leonhardt, *Essential quantum optics: from quantum measurements to Black Holes*, vol. 67. Cambridge University Press, 2010.

[24] W. Unruh, "Quantum Noise in Amplifiers and Hawking/Dumb-Hole Radiation as Amplifier Noise," arXiv:1107.2669 [gr-qc].

[25] M. Abramowitz and I. Stegun, *Handbook of mathematical functions with formulas, graphs, and mathematical tables*, vol. 55. Dover publications, 1964.

[26] J. Chaline, G. Jannes, P. Maissa, and G. Rousseaux, "Some aspects of dispersive horizons: lessons from surface waves," arXiv:1203.2492 [physics.flu-dyn].

[27] S. Finazzi and R. Parentani, "Spectral properties of acoustic black hole radiation: broadening the horizon," *Phys. Rev.* **D 83** (2011) 084010, arXiv:1012.1556 [gr-qc].

[28] V. Fleurov and R. Schilling, "Regularization of fluctuations near the sonic horizon due to the quantum potential and its influence on Hawking radiation," *Phys. Rev.* **A 85** (2012) 045602, arXiv:1105.0799 [cond-mat.quant-gas].

[29] N. Van Kampen, *Stochastic processes in physics and chemistry*, vol. 1. North holland, 1992.

[30] A. Coutant, *Stability properties of Hawking radiation in the presence of ultraviolet violation of local Lorentz invariance*. PhD thesis, Université Paris-Sud 11, 2012.